Theoretical and Applied Genetics (2020) 133:395–407
https://doi.org/10.1007/s00122-019-03470-6

ORIGINAL ARTICLE

Two tightly linked genes coding for NAD-dependent malic enzyme and dynamin-related protein are associated with resistance to Cercospora leaf spot disease in cowpea (*Vigna unguiculata* (L.) Walp.)

Titnarong Heng[1] · Akito Kaga[2] · Xin Chen[3] · Prakit Somta[1,4]

Received: 4 May 2019 / Accepted: 28 October 2019 / Published online: 6 November 2019

Abstract

Cercospora leaf spot (CLS) caused by *Cercospora canescens* is an important disease of cowpea (*Vigna unguiculata*). A previous study using an F_2 population [CSR12906 (susceptible) × IT90K-59-120 (resistant)] identified a major QTL *qCLS9.1* for resistance to CLS. In this study, we finely mapped and identified candidate genes of *qCLS9.1* using an $F_{3:4}$ population of 699 individuals derived from two $F_{2:3}$ individuals segregating at *qCLS9.1* from the original population. Fine mapping narrowed down the *qCLS9.1* for the resistance to a 60.6-Kb region on cowpea chromosome 10. There were two annotated genes in the 60.6-Kb region; *Vigun10g019300* coding for NAD-dependent malic enzyme 1 (NAD-ME1) and *Vigun10g019400* coding for dynamin-related protein 1C (DRP1C). DNA sequence analysis revealed 12 and 2 single nucleotide polymorphisms (SNPs) in the coding sequence (CDS) and the 5′ untranslated region and TATA boxes of *Vigun10g019300* and *Vigun10g019400*, respectively. Three SNPs caused amino acid changes in NAD-ME1 in CSR12906, N299S, S488N and S544N. Protein prediction analysis suggested that S488N of CSR12906 may have a deleterious effect on the function of NAD-ME1. Gene expression analysis demonstrated that IT90K-59-120 and CSR12906 challenged with *C. canescens* showed different expression in both *Vigun10g019300* and *Vigun10g019400*. Taken together, these results indicated that *Vigun10g019300* and *Vigun10g019400* are the candidate genes for CLS resistance in the cowpea IT90K-59-120. Two derived cleaved amplified polymorphic sequence markers were developed to detect the resistance alleles at *Vigun10g019300* and *Vigun10g019400* in IT90K-59-120.

Introduction

Cowpea (*Vigna unguiculata* (L.) Walp.) is one of the most important legume crops globally. It is widely grown in tropical and subtropical regions, especially in Africa and Asia. Four groups or subspecies of cultivated cowpea are generally recognized, including grain cowpea (ssp. *unguiculata*), yardlong bean (ssp. *sesquipedalis* (L.) Verdc.), biflora/catjang bean (ssp. *cylindrica* (L.) Verdc.) and textilis (ssp. *textilis* (L.) Verdc.) (Singh 2005). Among them, grain cowpea and yardlong bean are the most popular for cultivation. These crops have highly contrasting morphological and physiological characteristics. Grain cowpea (also known as black-eye pea) is usually cultivated for its dry seed, although its young pods are also consumed as a vegetable. Yardlong bean (also known as asparagus bean) is cultivated chiefly for its long-tender-young pods. Pods of grain cowpea are about 15–35 cm in length, while pods of yardlong bean are about 30–120 cm in length (Singh 2005). Grain cowpea is

Communicated by Mathew N. Nelson.

Electronic supplementary material The online version of this article (https://doi.org/10.1007/s00122-019-03470-6) contains supplementary material, which is available to authorized users.

✉ Prakit Somta
agrpks@ku.ac.th

[1] Department of Agronomy, Faculty of Agriculture at Kamphaeng Saen, Kasetsart University, Kamphaeng Saen, Nakhon Pathom 73140, Thailand

[2] Soybean and Field Crop Applied Genomics Research Unit, Institute of Crop Science, National Agriculture and Food Research Organization, 2-1-2, Kannondai, Tsukuba, Ibaraki 305-8602, Japan

[3] Institute of Industrial Crops, Jiangsu Academy of Agricultural Sciences, Nanjing 210014, Jiangsu, China

[4] Center of Excellence on Agricultural Biotechnology: (AG-BIO/PERDO-CHE), Bangkok 10900, Thailand

principally cultivated in Africa, whereas yardlong bean is mainly cultivated in Asia and is a chief source of protein for people in developing counties. Young pods of yardlong bean are consumed as a vegetable in several ways in both raw and cooked forms and thus provide dietary minerals, vitamins and fibers. The young pods can be harvested several times beginning at about 45–50 days after sowing (Kongjaimun et al. 2012). In general, compared with grain cowpea, yardlong bean needs wetter and cooler environments to thrive. However, grain cowpea appears to be more resistant to biotic and abiotic stresses than yardlong bean.

Fungal disease is one of the main biotic stresses affecting the growth, development and yielding of cowpea (Singh 2005). Cercospora leaf spot (CLS) disease caused by *Cercospora canescens* Ellis and Martin or *Pseudocercospora cruenta* (Sacc.) Deighton (Crous and Braun 2003; Deighton 1976) is one of the important fungal diseases of cowpea. CLS disease widely occurs in the tropical and subtropical regions, especially in the rainy season when high moisture levels and warm temperatures prevail. The leaf spot symptoms of *C. canescens* are circular, while those of *P. cruenta* are angular. *C. canescens* is comparatively a weaker parasite than *P. cruenta*, but it has a wider host range under tropical climates (Fery et al. 1976). The fungi start to affect cowpea plants from the beginning of the flowering stage onwards. The disease can cause yield loss from 35 to 40% in susceptible varieties (Schneider et al. 1976; Fery et al. 1976). In yardlong bean, the spot symptom also appears on young pods, resulting in them becoming unmarketable. Yardlong bean is more susceptible to CLS disease than grain cowpea because field cultivation of yardlong bean requires higher soil moisture content (more irrigation) and the large bushy canopy creates more shading (Duangsong et al. 2016). Thus, enhancement of resistance to CLS is a major objective in yardlong bean breeding programs.

To date there have been some reports published on the genetics of resistance to CLS disease in grain cowpea. Genetic studies revealed that the resistance to CLS disease caused by *P. cruenta* is controlled by a single dominant gene (Fery et al. 1976; Castro et al. 2003) or single recessive gene (Fery et al. 1976) or oligogenes or polygenes (Booker and Umaharan 2008) depending on resistance sources. The single-dominant gene and the single-recessive gene for the resistance are designated as *Cls1* and *cls2*, respectively. These two genes are not linked (Fery and Dukes 1977).

Recently, we reported that resistance to CLS disease caused by *C. canescens* and *P. cruenta* in the grain cowpea breeding line IT90K-59-120 is controlled by a single gene based on segregation and quantitative analyses (Duangsong et al. 2016; 2018). In addition, a major QTL for the resistance, *qCLS9.1*, in IT90K-59-120 was identified (Duangsong et al. 2016). *qCLS9.1* is located in a region of 3.5 cM on linkage group 9 (LG9; corresponding to chromosome 10 of the cowpea reference sequence) between simple sequence repeat (SSR) markers CEDG070 and CEDG304. It accounted for up to about 90% and 30% of the disease variation caused by *C. canescens* and *P. cruenta*, respectively (Duangsong et al. 2016). In addition, *qCLS9.1* is possibly the same locus as *ALS10.1*, which is a major QTL conferring resistance to angular leaf spot disease caused by *P. griseola* (Sacc.) Crous and U. Braun in common bean [*Phaseolus vulgaris* (L.)] (Oblessuc et al. 2015). Therefore, *qCLS9.1* for the resistance to CLS is interesting. In this study, we reported fine mapping and identification of candidate genes for *qCLS9.1* conferring CLS resistance in IT90K-59-120.

Materials and methods

Plant materials and population development

As the *qCLS9.1* was localized to the interval between SSR markers CEDG070 and CEDG304 on LG9 using an $F_{2:3}$ population developed from the cross CSR12906 × IT90K-59-120 (Duangsong et al. 2016), an $F_{2:3}$ family segregating for the QTL *qCLS9.1* was selected based on the marker genotype of CEDG070 being 0.5 cM from the *qCLS9.1* and disease scores of its F_2 ancestor plant (#80). This F_2 plant showed a heterozygous genotype at the marker CEDG070, but showed homozygous genotypes at all the other markers on the LG9. Twenty-three F_3 plants derived from self-pollination of the #80 F_2 plant were grown and genotyped with CEDG070 in which two plants showing heterozygosis at this marker were selected and self-pollinated to generate an $F_{3:4}$ population segregating at *qCLS9.1* as a mapping population. The original F_2 population used to identify *qCLS9.1* (Duangsong et al. 2016) was also used in this study to confirm the QTL(s) identified by fine mapping.

DNA extraction and valuation for disease resistance

The $F_{3:4}$ population was used to evaluate resistance to CLS disease. In total, 699 $F_{3:4}$ individuals and their parental lines (IT90K-59-120 and CSR1906) were grown during August to October 2017 (rainy season) under field conditions in Paktho District, Ratchaburi Province, Thailand, which is a hot spot for CLS disease in yardlong bean in Thailand (Duangsong et al. 2016). The space between plants and rows was 50 and 50 cm, respectively. Each row contained 80 individuals. The susceptible parent CSR1906 was grown around the experimental field as a natural source of CLS inoculums. Fifteen days after planting (DAP), young leaves from each plant were collected and extracted for genomic DNA following a CTAB method described by Lodhi et al. (1994).

At 40 and 50 DAP, the $F_{3:4}$ and parental plants were inoculated with *C. canescens* as per the procedures described

by Chankaew et al. (2011), which were the same as those used by Duangsong et al. (2016). Before inoculation, conidia taken from infected plants were examined using a light microscope to confirm that the disease symptoms were the result of infection by *C. canescens*. At 20 and 30 days after inoculation, CLS disease symptoms on leaves of each tested plant were scored. The scoring was carried out by three trained staff using the disease rating scale of 1–5 where 1 = no visual disease infection, 2 = 1–25% leaf area infected, 3 = 26–50% leaf area infected, 4 = 51–75% leaf area infected and 5 = 76–100% leaf area infected.

Development of new SSR markers for fine mapping *qCLS9.1*

The QTL *qCLS9.1* region was delimited by SSR markers PvM13 and CEDG304 (Duangsong et al. 2016). The location of these markers on the cowpea reference genome was determined by conducting a BLASTN search of the sequences of these markers against the cowpea reference genome in the Phytozome database (https://phytozome.jgi.doe.gov/pz/portal.html#!info?alias=Org_Vunguiculata_er) (Muñoz-Amatriaín et al. 2017; Lonardi et al. 2019). Once the physical genome locations of the PvM13 and CEDG304 were identified, DNA sequences between these two locations were downloaded and then searched for SSR sequences using SSRIT software (Temnykh et al. 2001). Primers for the SSRs were designed using Primer3 software (Untergasser et al. 2012) (Supplementary Table S1) and used to screen for polymorphisms between CSR12906 and IT90K-59-120. SSR analysis was carried out as per Duangsong et al. (2016) with minor modifications. Briefly, PCR was carried out in a total volume of 10 µL containing 5 ng of DNA template, 1 × *Taq* buffer, 2 mM $MgCl_2$, 0.2 mM dNTPs, 1 U *Taq* DNA polymerase (Thermo Fisher Scientific) and 2.5 µM each of forward and reverse primers. Amplification was performed in a GeneAmp PCR 9700 System thermocycler (Applied Biosystems) programmed as follows: 94 °C for 2 min followed by 35 cycles of 94 °C for 30 s, 55 °C for 30 s, 72 °C for 1 min, and 72 °C for 10 min. PCR products were electrophoresed on 5% polyacrylamide gel electrophoresis and visualized by silver staining. Nine markers showing polymorphism between the parents were selected and used to genotype the $F_{3:4}$ population.

Linkage map construction and QTL analysis

Genotypes of nine polymorphic markers were used to construct a genetic linkage map using QTL IciMapping 4.1 software (Meng et al. 2015). The markers were grouped with a minimum logarithm of the odds (LOD) value of 3.0. Markers on the linkage group were ordered using the REcombination Counting and ORDering (RECORD) algorithm (van Os et al. 2005). The marker orders were rippled using the Sum of Adjacent Recombination Frequencies (SARF) function (Falk 1989). Recombination frequencies were converted into genetic distance using the Kosambi mapping function (Kosambi 1944).

Location of the QTL *qCLS9.1* was determined by inclusive composite interval mapping (ICIM) (Li et al. 2007) using the same software as for the linkage analysis. ICIM was performed at every 0.1 cM. Significant LOD score threshold for the QTL was determined by running a 10,000-permutation test at $p = 0.001$. As the LOD graph indicated the possibility of the existence of two tightly linked QTLs for the resistance (see "Results"), a two-linked QTL model was tested using MultiQTL software (http://www.multiQTL.com) as described by Peng et al. (2003). A single QTL model and two-linked QTL model were tested by comparing hypotheses with a single QTL present (H_1) with no QTL (H_0) and two-linked QTLs (H_2) to the H_0, respectively. Then, the H_2 was compared to the H_1 using a 1000-permutation test to ensure whether the two-linked QTL model fit the data better than the single QTL model.

Confirming QTL(s) for the resistance

The QTLs identified by fine mapping in the $F_{3:4}$ population were confirmed in the original F_2 population of 190 individuals segregating for *qCLS9.1* (Duangsong et al. 2016). The F_2 population was genotyped with the nine polymorphic markers used in the $F_{3:4}$ population. Marker analysis, linkage map construction and QTL detection were the same as described above.

Sequencing of candidate genes for *qCLS9.1*

After QTL analysis, the reference genome location of the QTL regions was inspected to find candidate genes for *qCLS9.1*. Annotated genes located between the markers flanking the QTL(s) were considered as candidate gene(s) for CLS resistance. Primers were designed to the downloaded reference sequence to amplify the full transcript sequence and upstream sequence of the candidate gene(s) using Primer3 (Supplementary Table S2). cDNA (see "Expression analysis of the candidate genes" section) and genomic DNA of CSR12906 and IT90K-59-120 were amplified using the primers designed for each candidate gene. PCR was carried out in a total volume of 10 µL containing 5 ng of DNA template, 1 × *Taq* buffer, 2 mM $MgCl_2$, 0.2 mM dNTPs, 1 U *Taq* DNA polymerase (Thermo Fisher Scientific) and 0.5 µM each of forward and reward primers. Amplification was performed in a GeneAmp PCR 9700 System thermocycler (Applied Biosystems) programmed as follows: 94 °C for 2 min followed by 35 cycles of 94 °C for 30 s, 55 °C for 1 min, 72 °C for 1 min, and 72 °C for

10 min. PCR products were run on 1.5% agarose gel electrophoresis to confirm the single DNA fragment amplified. The PCR products were sequenced by Sanger sequencing using an ABI 3730xl DNA analyzer with Big Dye Terminator v3.1 kit (Applied Biosystems, USA). Sequences were edited and assembled using Sequencher v5.4.6 (Gene Codes Corporation). The sequences of the CSR12906, IT90K-59-120 and reference sequence were aligned to identify nucleotide polymorphism(s) that may cause amino acid change. The cDNA sequences of CSR12906, IT90K-59-120 were translated into protein sequences and aligned to find amino acid polymorphisms. The effect of amino acid change in the protein was predicted by using Protein Variation Effect Analyzer (PROVEAN) software (Choi et al. 2012). The significant threshold PROVEAN value was set at 2.5. If the PROVEAN value is above this threshold, it is predicted to have a deleterious effect on protein function.

Development of allele-specific markers for candidate genes

The SNPs between parental lines identified in the candidate gene(s) were used to develop cleaved amplified polymorphic sequence (CAPS) (Konieczny and Ausubel 1993) or derived cleaved amplified polymorphic sequence (dCAPS) markers (Neff et al. 1998). Primers for CAPS and dCAPS were designed to amplify SNP regions using Primer3 and dCAPS Finder 2.0 (Neff et al. 2002), respectively (Supplementary Table S4). PCR amplification was conducted in the parental lines using the same procedure as described above. PCR products were run on 1.5% agarose gel electrophoresis to confirm the single DNA fragment amplified. The PCR products were digested with FastDigest *Rsa*I restriction enzyme (Thermo Scientific), which recognizes GT^AC, at 37 °C for 15 min. After cutting, the PCR products were run on 3.0% agarose gel electrophoresis and stained with ethidium bromide for visualization.

Expression analysis of the candidate genes

CSR12906 and IT90K-59-120 were grown in field conditions at Kasetsart University, Kamphaeng Saen Campus, Nakhon Pathom, Thailand, during September to October 2018 (rainy season). Forty days after planting, the plants were inoculated with spore suspensions of *Cercospora canescens*. At 0, 2, 4, 6, 12, 24 and 48 h post-inoculation (hpi), leaves were collected and extracted for total RNA following the protocol described by Laksana and Chanprame (2015). The RNA was treated with DNA-free™ DNaseI (Ambion) and converted to cDNA using a RevertAid H Minus First Strand cDNA Synthesis Kit (Thermo Scientific) according to the manufacturer's instructions. cDNA concentration was quantified using a ND-1000 Spectrophotometer (NanoDrop Technologies Inc.). The cDNA was subjected to gene expression analysis by quantitative real-time polymerase chain reaction (qRT-PCR). Primers for qRT-PCR of candidate genes and *ACTIN* (*Vigun07g025200*) were designed using Primer3 (Supplementary Table S3). qRT-PCR was performed using ViiA 7 Real-Time PCR System (Applied Biosystems). Three biological and technical replicates were conducted for each sample. Reaction mixtures contained water, 1 × Master mix of Fast SYBR™ Green Master Mix (Thermo Fisher Scientific), 5 µM of forward primer, 5 µM of reverse primer and 50 ng cDNA. Thermocycler conditions included initial denaturation at 95 °C for 20 s, followed by 40 cycles at 95 °C for 3 s and 60 °C for 30 s. After 40 cycles, a melting curve was generated by slowly increasing (0.5 °C per 1 s) the temperature from 60 to 95 °C while the fluorescence was measured. Fluorescent data were acquired during each extension phase. Expression levels of *Vigun10g019300* and *Vigun10g019400* were calculated based on the ΔC_T method by using reference gene (*ACTIN*) (Livak and Schmittgen 2001).

Results

Response to CLS disease in the $F_{3:4}$ population

Parental line and $F_{3:4}$ plant responses to CLS disease were scored at 70 DAP. The yardlong bean CSR12906 was highly susceptible to the disease with a disease score of 4.50, while cowpea IT90K-59-120 was highly resistant with a disease score of 1.20. The disease scores of the $F_{3:4}$ plants showed continuous distribution and ranged from 1.00 to 5.00 with a mean of 3.72 (Fig. 1).

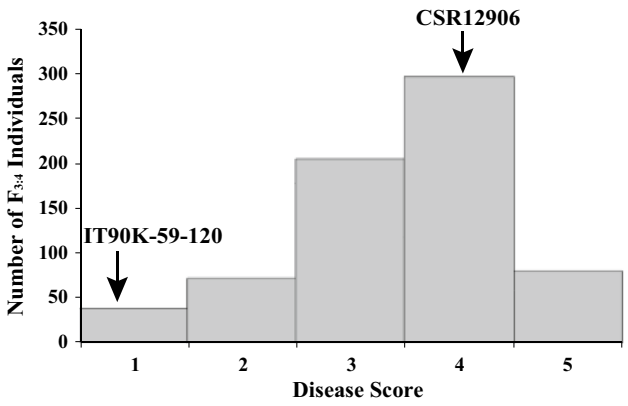

Fig. 1 Frequency distribution of disease score for Cercospora leaf spot disease caused by *Cercospora canescens* in a cowpea $F_{3:4}$ population of 699 individuals from the cross CSR12906 × IT90K-59-120

Fine mapping for *qCLS9.1* and confirmation of the QTLs for CLS resistance

The locations of PvM13 and CEDG304, in which SSR markers delimited the QTL *qCLS9.1* region in the previous study (Duangsong et al. 2016), were 34.03 and 22.51 Mbp (11.52 Mbp) on chromosome 10 of the cowpea reference genome, respectively. Among 70 newly developed SSR markers residing in this region, 47 were able to amplify DNA of CSR12906 and IT90K-59-120 and 17 were polymorphic markers between these two cowpea lines. A linkage map constructed based on the eight new polymorphic markers and CEDG070 for the $F_{3:4}$ population spanned 25.84 cM in length. All the marker orders completely agreed with their position on the cowpea reference sequence.

QTL analysis in the $F_{3:4}$ population revealed that two tightly linked QTLs, named *qCLS9.1A* and *qCLS9.1B*, are involved in CLS resistance (Table 1 and Fig. 2). *qCLS9.1A* was located at 15.30 cM between markers VU10g3-11 and VU10g3-12, while *qCLS9.1B* was located at 20.10 cM between markers CEDG070 and VU10g3-14. *qCLS9.1A* showed a LOD score of 44.76 and accounted for 23.45% of the disease score variation in the $F_{3:4}$ population. It possessed an additive effect of 0.53 and a dominant effect of 0.01. *qCLS9.1B* showed a LOD score of 60.76 and explained 33.72% of the disease score variation in the $F_{3:4}$ population. It had additive and dominant effects of 0.65 and 0.03, respectively. At both *qCLS9.1A* and *qCLS9.1B*, allele(s) from IT90K-59-120 decreased the disease score (elevated the resistance). The existence of the tightly linked QTLs *qCLS9.1A* and *qCLS9.1B* was also supported by the two-linked QTL model created using MultiQTL (Supplementary Table S5). Genotypic analysis revealed that plants possessing IT90K-59-120 homozygous alleles at both *qCLS9.1A* and *qCLS9.1B* are highly resistant with disease scores < 2.0, those possessing IT90K-59-120 homozygous alleles at *qCLS9.1A* or *qCLS9.1B* are moderately resistant with disease scores of about 2.5–3.0, and those possessing CSR12906 homozygous alleles at both *qCLS9.1A* and *qCLS9.1B* are highly susceptible with disease scores > 3.50 (Fig. 2b).

The QTLs identified by fine mapping using the $F_{3:4}$ population were re-analyzed using a linkage map constructed with the same markers for the original F_2 population reported by Duangsong et al. (2016) in which disease scoring was conducted at 60 and 70 DAP. In the present study, QTL analysis consistently identified one QTL, *qCLS9.1A,* for the resistance at both 60 and 70 DAP. *qCLS9.1A* was located between markers PvM127 and VU10g3-9 (Table 2 and Supplementary Fig. S7). *qCLS9.1A* accounted for more than 80% of the disease score variation in the $F_{2:3}$ population. The QTL possessed an additive effect of 0.94–1.44 and a dominant effect of nearly 0.

Identification of candidate genes for *qCLS9.1A* and *qCLS9.1B*

Based on the cowpea reference genome version 1.1, the physical region of marker interval VU10g3-9–VU10g3-14 covering *qCLS9.1A* and *qCLS9.1B* in the fine mapping population is only 60.6 Kbp (Fig. 2c). There are two annotated genes in this region: *Vigun10g019300* and *Vigun10g019400*. *Vigun10g019300* is located on the interval between markers VU10g3-11 and VU10g3-12, while *Vigun10g019400* is between markers VU10g3-12 and CEDG070. In fact, VU10g3-11 is a part of *Vigun10g019300*, while CEDG070 is a part of *Vigun10g019400*. The distance between *Vigun10g019300* and *Vigun10g019400* is only 10.3 Kbp. *Vigun10g019300* encodes NAD-dependent malic enzyme 1 (NAD-ME1), while *Vigun10g019400* encodes for dynamin-related protein 1C (DRP1C). *Vigun10g019400* is a homolog to AtDRP1E [known as enhanced disease resistance 3 (EDR3)]. These genes are considered as candidate genes for *qCLS9.1A* and *qCLS9.1B*, respectively, explaining the CLS resistance in IT90K-59-120.

Nucleotide and amino acid variations in *Vigun10g019300* and *Vigun10g019400*

Transcript and upstream sequences of *Vigun10g019300* and *Vigun10g019400* were determined for CSR12906 and IT90K-59-120. The sequence alignment of *Vigun10g019300* transcripts revealed 12 SNPs between CSR12906 and IT90K-59-120. Upstream sequence alignment of *Vigun10g019300* showed one SNP in the 5′ untranslated region (UTR) (Supplementary Fig. S1). SNPs at positions 896, 1464 and 1631 in the CDS, corresponding to positions 18,642, 30,562 and 35,574 of the open reading frame (ORF), respectively, (Fig. 3a) cause the amino acid change at positions 299 aa (N → S), 488 aa (S → N) and 544 aa (S → N) of the CSR12906 NAD-ME1 protein, respectively (Fig. 4). cDNA sequence alignment of *Vigun10g019400* revealed one SNP between CSR12906 and IT90K-59-120 (Fig. 3b). This SNP was located at position 1608 (corresponding to position 6146 of the ORF) but did not cause amino acid change (Supplementary Fig. S5). However, upstream sequence alignment of this gene revealed one SNP in the 5′ UTR and two SNPs in the TATA boxes (Fig. 5 and Supplementary Fig. S3).

The effect of amino acid changes on the function of NAD-ME1 encoded by *Vigun10g019300* was predicted using PROVEAN software. Among the three amino acid changes in NAD-ME1, only the S488N change in CSR12906 possibly has a deleterious effect on the protein function. This amino acid change had a PROVEAN score of − 2.896, which is predicted to have a deleterious effect on protein function.

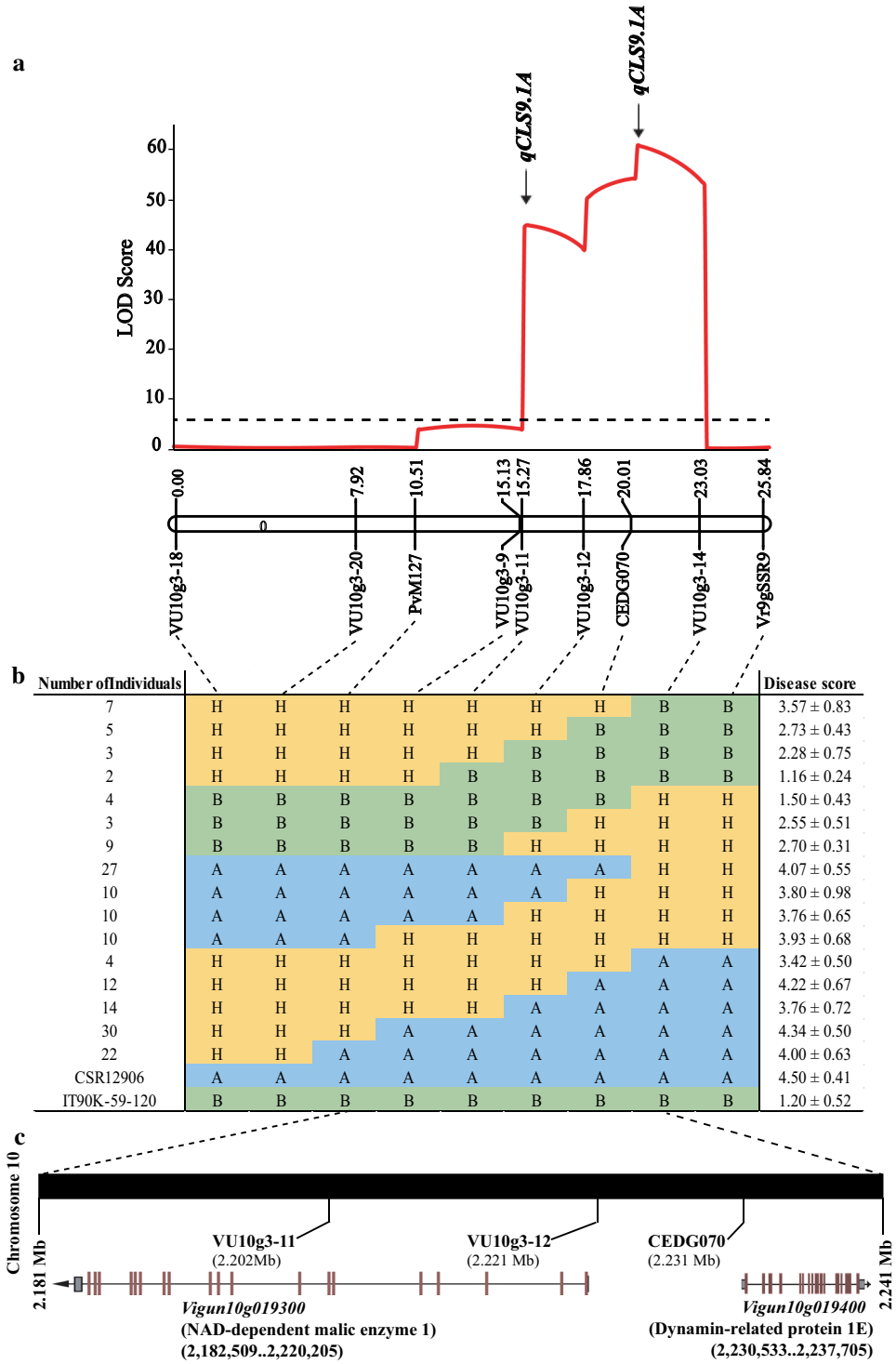

Fig. 2 Fine mapping of *qCLS9.1A* and *qCLS9.1B* for resistance to Cercospora leaf spot (CLS) disease caused by *C. canescens* using the $F_{3:4}$ population of the cross CSR12906 × IT90K-59-120. The LOD graph of QTLs (**a**). Dotted line parallel to the *X*-axis represents the LOD threshold for the QTLs. Marker genotypes and disease scores of CSR12906, IT90K-59-120 and 16 selected $F_{3:4}$ individuals carrying crossovers around *qCLS9.1A* and *qCLS9.1B* (**b**). The individuals carrying genotype B on both markers VU10g3-11 and CEDG070 are classified as highly resistant to CLS disease. Those individuals carrying genotype B on marker VU10g3-11 or CEDG070 are classified as moderately resistant to CLS disease. Any individuals carrying genotype A or H on both markers VU10g3-11 and CEDG070 are classified as susceptible to CLS disease. Physical locations of candidate genes and markers at QTLs *qCLS9.1A* and *qCLS9.1B* on the cowpea reference genome (**c**)

Differences in gene expression patterns of the candidate genes in parent lines

Gene expression of *Vigun10g019300* and *Vigun10g019400* in IT90K-59-120 and CSR12906 was measured by qRT-PCR at 0, 2, 4, 6, 12, 24 and 48 hpi. The expression level of *Vigun10g019300* between IT90K-59-120 and CSR12906 was significantly different at 4, 6 and 12 hpi (Fig. 6a). IT90K-59-120 showed higher expression than CSR12906 at 4 and 6 hpi, and the difference was pronounced at 6 hpi, whereas CSR12906 showed higher expression than IT90K-59-120 at 2, 12 and 24 hpi. The expression level of *Vigun10g019400* of IT90K-59-120 was significantly higher than that of CSR12906 at 4, 6, 12 and 48 hpi. The highest

Table 1 Positions and effects of QTLs controlling Cercospora leaf spot disease caused by *Cercospora canescens* confirmed in a cowpea F_2 population of 190 individuals from the cross CSR12906 × IT90K-59-120

Trait	QTL name	Position (cM)	Marker interval	LOD score	PVE (%)	Additive effect	Dominant effect
Disease score at 60 DAP	*qCLS9.1A*	6.00	PvM127–VU10g3-9	67.21	82.91	0.94	0.00
Disease score at 70 DAP	*qCLS9.1A*	6.00	PvM127–VU10g3-9	82.58	87.43	1.44	− 0.02

Disease scoring was conducted at 60 and 70 days after planting (DAP). The disease resistance was evaluated using a rating scale of 1 (highly resistant) to 5 (highly susceptible)

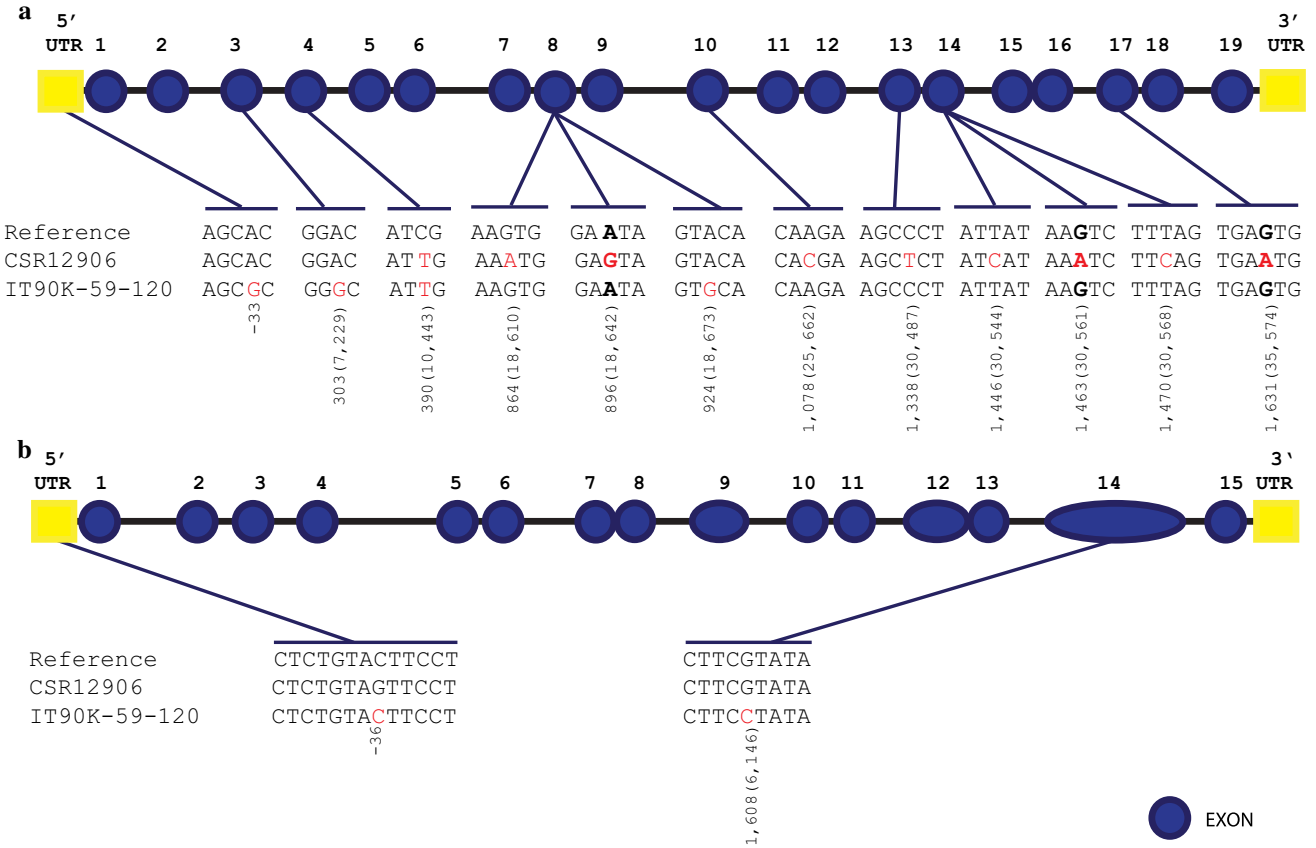

Fig. 3 Single nucleotide polymorphisms (SNPs) among CSR12906, IT90K-59-120 and cowpea reference genome sequence in *Vigun10g019300* (**a**) and *Vigun10g019400* (**b**). Number in parentheses under each SNP indicates its position in the open reading frame sequence. SNPs causing amino acid changes are in bold

expression was at 6 hpi, followed by 4 and 12 hpi, respectively (Fig. 6b).

Development of CAPS and dCAPS markers

CAPS marker cVU19300 and dCAPS marker dVU19400 were developed to detect the CDS SNP(s) at position 1078 (corresponding to position 25,662 of the ORF (position 2,208,171 on chromosome 10)) in *Vigun10g019300* and the CDS SNP at position 1608 (corresponding to position 6146 of the ORF (position 2,236,679 on chromosome 10)) in *Vigun10g019400*, respectively (Fig. 3). These SNPs are detected by the restriction enzyme *Rsa*I. dVU19300 primers amplified a fragment of 255, while dVU19400 primers amplified a region of 282. Analysis of CAPS marker cVU19300 revealed polymorphism between CSR12906 and IT90K-59-120. CSR12906 had three DNA bands of sizes 153, 70 and 32 bp, while IT90K-59-120 had two DNA bands of sizes 153 and 102 bp (Fig. 7a). $F_{3:4}$ individuals possessing heterozygous SNP at this marker had four DNA bands (Fig. 7a). Analysis of the dCAPS marker dVU19400 showed polymorphism between CSR12906 and IT90K-59-120. SR12906 and IT90K-59-120 showed a DNA band size of 255 bp and 282 bp, respectively (Fig. 7b). $F_{3:4}$ individuals

```
Reference         MAMLLKHVRASSSLLKQHVTRAHLLSRPFTTTEGHRPSIVHKRSLDILHDPWFNKGTAFS 60
CSR12906          MAMLLKHVRASSSLLKQHVTRAHLLSRPFTTTEGHRPSIVHKRSLDILHDPWFNKGTAFS 60
IT90K-59-120      MAMLLKHVRASSSLLKQHVTRAHLLSRPFTTTEGHRPSIVHKRSLDILHDPWFNKGTAFS 60
                  ************************************************************

Reference         MTERDRLDLRGLLPPNVMSPDLQIERFMVDLKRLEVQARDGPSDPYALAKWRILNRLHDR 120
CSR12906          MTERDRLDLRGLLPPNVMSPDLQIERFMVDLKRLEVQARDGPSDPYALAKWRILNRLHDR 120
IT90K-59-120      MTERDRLDLRGLLPPNVMSPDLQIERFMVDLKRLEVQARDGPSDPYALAKWRILNRLHDR 120
                  ************************************************************

Reference         NETMYYKVLIAKIEEYAPIVYTPTVGLVCQNYSGLFRRPRGMYFSAEDRGEMMSMVYNWP 180
CSR12906          NETMYYKVLIAKIEEYAPIVYTPTVGLVCQNYSGLFRRPRGMYFSAEDRGEMMSMVYNWP 180
IT90K-59-120      NETMYYKVLIAKIEEYAPIVYTPTVGLVCQNYSGLFRRPRGMYFSAEDRGEMMSMVYNWP 180
                  ************************************************************

Reference         AEQVDMIVVTDGSRILGLGDLGVQGIGIAIGKLDLYVAAAGINPQRVLPVMIDVGTNNEK 240
CSR12906          AEQVDMIVVTDGSRILGLGDLGVQGIGIAIGKLDLYVAAAGINPQRVLPVMIDVGTNNEK 240
IT90K-59-120      AEQVDMIVVTDGSRILGLGDLGVQGIGIAIGKLDLYVAAAGINPQRVLPVMIDVGTNNEK 240
                  ************************************************************

Reference         LLEDPLYLGLQQHRLDGDDYLAVVDEFMEAVFTRWPNVIVQFEDFQSKWAFKLLQRYRNT 300
CSR12906          LLEDPLYLGLQQHRLDGDDYLAVVDEFMEAVFTRWPNVIVQFEDFQSKWAFKLLQRYRST 300
IT90K-59-120      LLEDPLYLGLQQHRLDGDDYLAVVDEFMEAVFTRWPNVIVQFEDFQSKWAFKLLQRYRNT 300
                  ************************************************************.*

Reference         YRMFNDDVQGTAGVAIAGLLGAVRAQGRPMIDFPKQKIVVAGAGSAGIGVLNAARKTMAR 360
CSR12906          YRMFNDDVQGTAGVAIAGLLGAVRAQGRPMIDFPKQKIVVAGAGSAGIGVLNAARKTMAR 360
IT90K-59-120      YRMFNDDVQGTAGVAIAGLLGAVRAQGRPMIDFPKQKIVVAGAGSAGIGVLNAARKTMAR 360
                  ************************************************************

Reference         MLGNNEVAFESAKSQFWVVDAKGLISEGRENIDPDALPFARNLKEIERQGLREGASLEEV 420
CSR12906          MLGNNEVAFESAKSQFWVVDAKGLISEGRENIDPDALPFARNLKEIERQGLREGASLEEV 420
IT90K-59-120      MLGNNEVAFESAKSQFWVVDAKGLISEGRENIDPDALPFARNLKEIERQGLREGASLEEV 420
                  ************************************************************

Reference         VKQVKPDVLLGLSAVGGLFSKEVLEALKDSTSTRPAIFAMSNPTKNAECTAEEAFSILGD 480
CSR12906          VKQVKPDVLLGLSAVGGLFSKEVLEALKDSTSTRPAIFAMSNPTKNAECTAEEAFSILGD 480
IT90K-59-120      VKQVKPDVLLGLSAVGGLFSKEVLEALKDSTSTRPAIFAMSNPTKNAECTAEEAFSILGD 480
                  ************************************************************

Reference         NIIFASGSPFSNVDLGNGHIGHCNQGNNMYLFPGIGLGTLLSGARIISDGMLQAAAERLA 540
CSR12906          NIIFASGNPFSNVDLGNGHIGHCNQGNNMYLFPGIGLGTLLSGARIISDGMLQAAAERLA 540
IT90K-59-120      NIIFASGSPFSNVDLGNGHIGHCNQGNNMYLFPGIGLGTLLSGARIISDGMLQAAAERLA 540
                  *******.****************************************************

Reference         TYMSEEEVLKGIIFPSTSRIRDITEKVAAAVIKEALEEDLAEGYHGMDARELKKLSEDDL 600
CSR12906          TYMNEEEVLKGIIFPSTSRIRDITEKVAAAVIKEALEEDLAEGYHGMDARELKKLSEDDL 600
IT90K-59-120      TYMSEEEVLKGIIFPSTSRIRDITEKVAAAVIKEALEEDLAEGYHGMDARELKKLSEDDL 600
                  ***.********************************************************

Reference         AEFVKNNMWNPEYPTLVYKKE* 621
CSR12906          AEFVKNNMWNPEYPTLVYKKE* 621
IT90K-59-120      AEFVKNNMWNPEYPTLVYKKE* 621
                  **********************
```

Fig. 4 Alignment of amino acid sequences of NAD-dependent malic enzyme 1 encoded by *Vigun10g019300* in CSR12906, IT90K-59-120 and the cowpea reference genome. Asterisk (*) indicates fully conserved residue. Period (.) indicates conservation between amino acids of weakly similar properties

possessing a heterozygous SNP at the marker dVU19400 showed two DNA bands (Fig. 7b).

Discussion

Previous study using qualitative and quantitative genetic analyses demonstrated that the CLS resistance in IT90K-59-120 is controlled by a single gene (Duangsong et al. 2018). Duangsong et al. (2016) showed that *qCLS9.1* is a major QTL controlling CLS resistance in this cowpea. Based on the cowpea reference sequence (Muñoz-Amatriaín et al. 2017; Lonardi et al. 2019), the markers CEDG070 and CEDG304 flanking *qCLS9.1* are 20.28 Mbp apart and contain 613 genes. In this study, by analyzing newly developed SSRs in a population segregating at only *qCLS9.1* originating from an F_2 plant in the mapping population (CSR12906 × IT90K-59-120) used by Duangsong et al. (2016), we successfully narrowed down the *qCLS9.1* to a 60.6-Kbp region on chromosome 10 of cowpea (Fig. 2). In

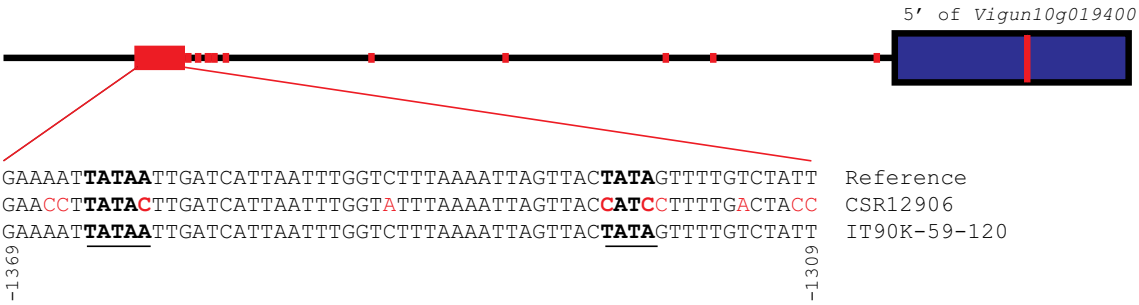

Fig. 5 Single nucleotide polymorphisms (SNPs) in the upstream region of *Vigun10g019400* in CSR12906, IT90K-59-120 and the cowpea reference genome. Portions and letters in red indicate the location of SNPs between CSR12906, IT90K-59-120 and the cowpea reference sequence. Letters and positions of TATA boxes are in bold and underlined

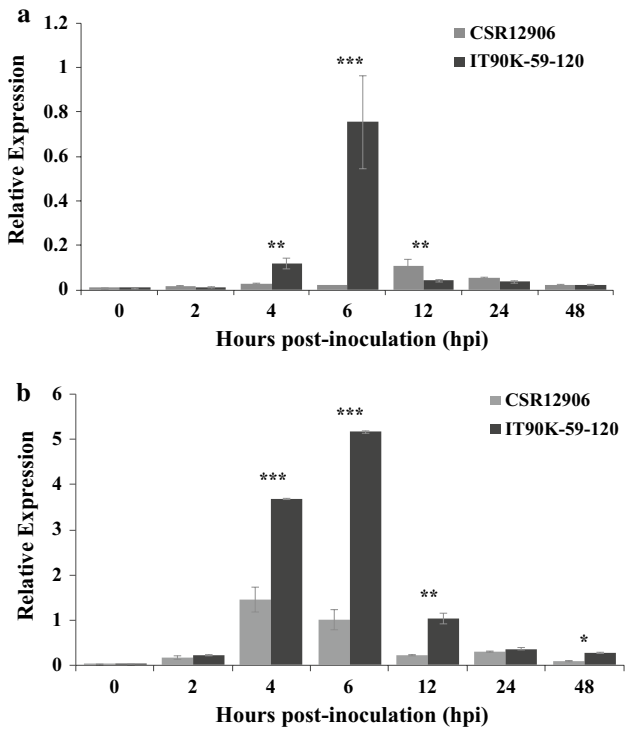

Fig. 6 Relative gene expression level of *Vigun10g019300* (**a**) and *Vigun10g019400* (**b**) in the leaves of CSR12906 and IT90K-59-120 at 0, 2, 4, 6, 12, 24 and 48 h post-inoculation (hpi) with *Cercospora canescens*. *, ** and *** indicate significant differences of gene expression level between CSR12906 and IT90K-59-120 by *t* test at $p=0.05$, $p=0.01$ and $p=0.001$, respectively

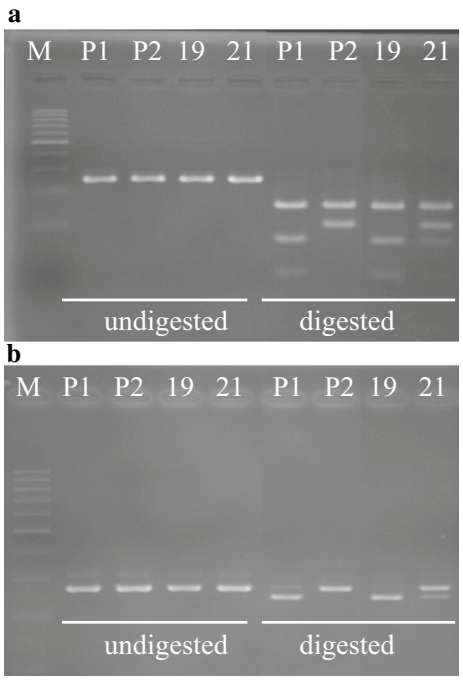

Fig. 7 DNA banding patterns of CAPS marker dVU19300 (**a**) and dCAPS marker dVU19400 (**b**). Amplified and digested DNA fragments with the restriction enzyme *Rsa*I were resolved by 3% agarose gel. M, 100 bp DNA ladder; P1, CSR12906; P2, IT90K-59-120; 19, $F_{3:4}$ individual number 19; 21, $F_{3:4}$ individual number 21

the present study, the previous *qCLS9.1* locus was found to be composed of two tightly linked major QTLs, *qCLS9.1A* and *qCLS9.1B* (Fig. 2a). However, the LOD graph of the 60.6-Kbp region did not clearly indicate the existence of the two QTLs and it is also possible that only one strong QTL exists. Evaluation of many recombinants from a larger population size may be able to unambiguously resolve if one or two QTLs exist in this narrow genome region. In the 60.6-Kbp region, however, there was no sequence gap in the cowpea reference sequence and the region contains only two annotated genes: *Vigun10g019300* coding for NAD-ME1 and *Vigun10g019400* coding for DRP1E (Fig. 2). As both *qCLS9.1A* and *qCLS9.1B* had comparable genetic effects that contribute to the CLS resistance (Table 1), the two genes were further characterized.

As compared with IT90K-59-120, NAD-ME1 in CSR12906 possesses three amino acid changes: N299S, S488N and S544N (Figs. 3a and 4 and Supplementary Fig.

Table 2 Positions and effects of QTLs controlling Cercospora leaf spot disease caused by *Cercospora canescens* in a cowpea $F_{3:4}$ population of 699 individuals from the cross CSR12906 × IT90K-59-120

QTL name	Position (cM)	Marker interval	LOD score	PVE (%)	Additive effect	Dominant effect
qCLS9.1A	15.30	VU10g3-11–VU10g3-12	44.76	23.45	0.53	0.01
qCLS9.1B	20.10	CEDG070–VU10g3-14	60.76	33.72	0.65	0.03

The disease resistance was evaluated using a rating scale of 1 (highly resistant) to 5 (highly susceptible)

S2). S488N was predicted to cause a deleterious effect on the NAD-ME1 function in CSR12906. Based on the Phytozome database, S488 locates in the NAD binding domain of NAD-ME1. Sequence alignment of NAD-ME1 proteins from cowpea, azuki bean (*Vigna angularis* (Ohwi) Ohwi and Ohashi), mungbean (*Vigna radiata* (L.) Wilczek), common bean (*Phaseolus vulgaris* L.), soybean (*Glycine max* (L.) Merr.), pigeon pea (*Cajanus cajan* (L.) Millsp.) and barrel medick (*Medicago truncatula* Gaertner) showed perfect conservation of S488 and S544 in these legumes (Supplementary Fig. S6), suggesting that S at these positions is important in the function of NAD-ME1.

In plants, NAD-MEs are found in mitochondria (Winning et al. 1994). NAD-MEs are a primary regulatory enzyme for the metabolism of malate in plant mitochondria. NAD-MEs catalyze the oxidative decarboxylation of L-malate using NAD^+ as a coenzyme to generate pyruvate, CO_2 and NADH. In plants, NADP-dependent malic enzymes (NADP-ME), a very similar decarboxylating enzymes to NAD-MEs, play an important role in disease resistance through their involvement in production of NADPH by NADPH oxidases for synthesis of reactive oxygen species (ROS). Apoplastic ROS bursts generated in elicited plant cells are sufficiently cytotoxic to kill invading pathogens (Legendre et al. 1993; Chi et al. 2009; Park et al. 2013). In addition, ROS act as signaling molecules that activate plant defenses against pathogen invasion (Tenhaken et al. 1995; Jabs 1999; Torres 2010). In *Arabidopsis thaliana*, a *nadp-me2* mutant showed enhanced susceptibility toward pathogens *Colletotrichum higginsianum* (Voll et al. 2012), *Botrytis cinerea* and *Pseudomonas syringae* pv. *tomato* (*Pto*) DC3000 (Mhamdi and Noctor 2016). Singh et al. (2018) showed that rice blast fungus *Magnaporthe oryzae* secrete effector AVR-Pii to inhibit NADP-ME2-3 function in rice (*Oryza sativa* L.) and disrupt host immunity. Malate has been reported to participate in plant disease resistance (Bolwell et al. 2002; Finkemeier et al. 2013), although its specific function in disease resistance is not known. To date there have been no reports on the direct involvement of NAD-ME in plant disease resistance, despite it having been shown that transgenic arabidopsis overexpressing OsNAD-ME1 exhibit germination and growth advantages under salt, alkali, drought, and oxidative stress conditions, suggesting that NAD-ME1 plays an important role in plant responses to abiotic stresses (Zhou et al. 2012). However, as NAD-ME and NADP-ME function in a very similar fashion, NAD-ME may provide the plant resistance to pathogen invasion in the same way as NADP-ME. In addition, as the generation of $O_2^{\cdot-}$, the proximal mitochondrial ROS, within mitochondria depends critically on proton motive force, NADH/NAD^+ and $CoQH_2$/CoQ (reduced CoQ/coenzyme Q) ratios and the local O_2 concentration (Murphy 2009) and the NADH and NAD^+ pools depend partially on NAD-ME (Schertl and Braun 2014); therefore, production of mitochondrial ROS partially depends on NAD-ME. It is worth mentioning that the rate of ROS production increases at high NADH/NAD^+ ratios (Abdelwahid et al. 2007; Adam-Vizi and Chinopoulos 2006). Taken together, these results indicate that *Vigun10g019300* encoding functional NAD-ME1 increases resistance to CLS in grain cowpea IT90K-59-120. Moreover, expression of *Vigun10g019300* in IT90K-59-120 was higher than that in CSR12906 (Fig. 6a). Taken together, our results are the first line of evidence that show the involvement of NAD-ME in plant disease resistance.

Vigun10g019400 coding for DRP1E, a dynamin-related protein (DRP), was found to associate with the CLS resistance in IT90K-59-120. DRP1E localizes in mitochondria (Tang et al. 2006; Li et al. 2017). Dynamins and DRPs are members of a protein superfamily of GTPases that are involved in diverse membrane-related processes in prokaryotic and eukaryotic cells, including membrane fusion (such as mitochondrial fission), membrane scission, membrane protection and/or membrane stabilization (Jilly et al. 2018). Although the specific function of DRPs in plant disease resistance remains poorly understood, studies have revealed that DRPs are implicated in plant disease resistance (Tang et al. 2006; Smith et al. 2014; Leslie et al. 2016; Li et al. 2017; Wu et al. 2018). For example, induction of cell death (Tang et al. 2006; Li et al. 2017) and vesicular trafficking through the perception of pathogen-associated molecular pattern (PAMP)-triggered immunity signaling (Smith et al. 2014) and regulation of the trafficking of proteins involved in callose synthase and/or callose degradation (Leslie et al. 2016). In *Arabidopsis thaliana*, Tang et al. (2006) demonstrated that *dynamin-related protein 1e* (*drp1e*) enhances susceptibility to *B. cinerea*. Similarly, Smith et al. (2014) showed that loss of *Dynamin-related Protein 2B* (*DRP2B*) results in decreased *PATHOGENESIS-RELATED 1*

(*PR1*) mRNA levels in response to *bacterial* infection and thus increased susceptibility to virulent and avirulent *Pto* DC3000 strains. In rice, Li et al. (2017) showed that *DRP1E* regulates programmed cell death (PCD) via the control of cytochrome c release from mitochondria. In our case, although the predicted DRP1E proteins encoded by *Vigun10g019400* in IT90K-59-120 and CSR12906 were the same (Supplementary Fig. S5), qRT-PCR analysis showed that *Vigun10g019400* was expressed statistically higher in IT90K-59-120 than CSR12906 during *C. canescent* ingress (Fig. 6b). SNPs in TATA boxes of this gene are likely the cause of the differential expression (Fig. 5). Taken together, the above data suggest that the high expression of *Vigun10g019400* appears to enhance resistance in grain cowpea IT90K-59-120, possibly by increasing production of mitochondrial ROS.

Interestingly, both NAD-ME1 and DRP1E, which were associated with CLS resistance in this study, locate in mitochondria and their functions are involved in ROS production. DRP1E controls cytochrome c release from mitochondria (Li et al. 2017). Cytochrome c is a heme-containing redox protein active in electron transfer pathways, including the respiratory electron transport chain (ETC) (Alvarez-Paggi et al. 2017; Supplementary Fig. S8). The plant mitochondrial ETC core includes classical oxidoreductase complexes (complex I to IV), cytochrome c, ubiquinone (coenzyme Q) and alternative oxidoreductases (Schertl and Braun 2014). NAD-MEs are among the dehydrogenase enzymes in the ETC complex II (succinate dehydrogenase) in the mitochondrial matrix that transfer electrons in the form of NADH to the ETC in which the NADH is re-oxidized by complex I or the internal alternative NAD(P)H dehydrogenases (Schertl and Braun 2014). Malate is the prime precursor in complex II and is oxidized by NAD-MEs to produce pyruvate that is fed into the tricarboxylic acid cycle (Krebs cycle) (Schertl and Braun 2014). It has been proposed that complex II may function as a general sensor for PCD (Grimm 2013; Lemarie et al. 2011). In the respiratory ETC, the cytochrome c shuttles electrons from complex III (cytochrome c reductase) to complex IV (cytochrome c oxidase) (Alvarez-Paggi et al. 2017). Based on our findings and this information, NAD-ME1 and DRP1E appear to play an important role in the electron transfer pathways in plant mitochondria that regulate ROS production and PCD (Supplementary Fig. S8) and contribute to CLS resistance in grain cowpea IT90K-59-120.

Because both *Vigun10g019300* and *Vigun10g019400*, which are associated with CLS resistance, are linked in the coupling phase, selection for a highly resistant genotype would not be difficult in breeding materials. The SSR markers VU10g3-9 and VU10g3-11 located in *Vigun10g019300* and CEDG070 located in *Vigun10g019300* can be used with a very high degree of precision for MAS for both genes to reduce time and resources for the development of CLS-resistant cowpea cultivar(s). Apart from these SSR markers, CAPS marker dVU19300 and dCAPS marker dVU19400 developed in the present study would be useful for MAS because both markers are allele-specific, segregate in a co-dominant manner and can be detected with simple molecular laboratory facilities.

Acknowledgements This research was supported by the Graduate School Scholarship from The Graduate School, Kasetsart University (Fiscal year 2016–2017) and by the project "The Capacity Building of KU Students on Internationalization Program: KUCSI" of Kasetsart University. We thank Liwen Bianji, Edanz Group China (www.liwenbianji.cn/ac) for editing the English text of a draft of this manuscript.

Author contribution PS conceived the idea of this study, secured research funding and coordinated this study; PS and TH obtained and/or assisted in the maintenance of the plant materials; TH carried out all the experiments in this study; AK was involved in genotyping, gene expression analysis and cDNA sequencing. XC contributed reagents. TH, PS and AK analyzed data and wrote the manuscript. All authors approved the final version of the manuscript.

Availability of data and materials All information is specified in the manuscript or included as Additional Files.

Compliance with ethical standards

Conflict of interest On behalf of all authors, the corresponding author states that there is no conflict of interest.

Ethical standards The authors declare that the experiments comply with the current laws of the country in which they were carried out.

References

Abdelwahid E, Yokokura T, Krieser RJ, Balasundaram S, Fowle WH, White K (2007) Mitochondrial disruption in *Drosophila* apoptosis. Dev Cell 12:793–806

Adam-Vizi V, Chinopoulos C (2006) Bioenergetics and the formation of mitochondrial reactive oxygen species. Trends Pharmacol Sci 27:639–645

Alvarez-Paggi D, Hannibal L, Castro MA, Oviedo-Rouco S, Demicheli V, Tórtora V et al (2017) Multifunctional cytochrome c: learning new tricks from an old dog. Chem Rev 117:13382–13460. https://doi.org/10.1021/acs.chemrev.7b00257

Bolwell GP, Bindschedler LV, Blee KA, Butt VS, Davies DR, Gardner SL, Gerrish C, Minibayeva F (2002) The apoplastic oxidative burst in response to biotic stress in plants: a three-component system. J Exp Bot 53:1367–1376

Booker HM, Umaharan P (2008) Quantitative resistance to Cercospora leaf spot disease caused by *Pseudocercospora cruenta* in cowpea. Euphytica 162:167–177

Castro NR, Menezes GC, Coelho RSB (2003) Inheritance of cowpea resistance to Cercospora leaf spot. Fitopato Bras. 28:552–554

Chankaew S, Somta P, Sorajjapinun W, Srinives P (2011) Quantitative trait loci mapping of Cercospora leaf spot resistance in mungbean, *Vigna radiata* (L.). Mol Breed 28:255

Chi MH, Park SY, Kim S, Lee YH (2009) A novel pathogenicity gene is required in the rice blast fungus to suppress the basal defenses

of the host. PLoS Pathog 5:e1000401. https://doi.org/10.1371/journal.ppat.1000401
Choi Y, Sims GE, Murphy S, Miller JR, Chan AP (2012) Predicting the functional effect of amino acid substitutions and indels. PLoS ONE 7(10):e46688. https://doi.org/10.1371/journal.pone.0046688
Crous PW, Braun U (2003) *Mycospaerella* and its anamorphs: 1. Names published in Cercospora and Passalora. Centraalbureau voor Schimmelcultures (CBS), Utrecht
Deighton FC (1976) Studies on *Cercospora* and allied genera. Mycol Pap 1:140–168
Duangsong U, Kaewwongwal A, Somta P, Chankaew S, Srinives P (2016) Identification of a major QTL for resistance to Cercospora leaf spot disease in cowpea (*Vigna unguiculata* (L.) Walp.) revealed common genomic region with that for the resistance to angular leaf spot in common bean (*Phaseolus vulgaris* L.). Euphytica 209:199–207
Duangsong U, Laosatit K, Somta P, Srinives P (2018) Genetics of resistance to Cercospora leaf spot disease caused by *Cercospora canescens* and *Pseudocercospora cruenta* in yardlong bean (*Vigna unguiculata* ssp. *sesquipedalis*) × grain cowpea (*V. unguiculata* ssp. *unguiculata*) populations. J Genet 97:1451–1456
Falk CT (1989) A simple scheme for preliminary ordering of multiple loci: application to 45 cf families. Prog Clin Biol Res 329:17–22
Fery RL, Dukes PD (1977) An assessment of two genes for Cercospora leaf spot resistance in the Southern pea (*Vigna unguiculata* (L.) Walp.). J Hortic Sci 12:454–456
Fery RL, Dukes PD, Cuthbert FP Jr (1976) The inheritance of Cercospora leaf spot resistance in Southern pea (*Vigna unguiculata* (L.) Walp.). J Hortic Sci 101:148–149
Finkemeier I, König AC, Heard W, Nunes-Nesi A, Pham PA, Leister D, Fernie AR, Sweetlove LJ (2013) Transcriptomic analysis of the role of carboxylic acids in metabolite signaling in Arabidopsis leaves. Plant Physiol 162:239–253. https://doi.org/10.1104/pp.113.214114
Grimm S (2013) Respiratory chain complex II as general sensor for apoptosis. Biochim Biophys Acta 1827:565–572
Jabs T (1999) Reactive oxygen intermediates as mediators of programmed cell death in plants and animals. Biochem Pharmacol 57:231–245
Jilly R, Khan NZ, Aronsson H, Schneider D (2018) Dynamin-like proteins are potentially involved in membrane dynamics within chloroplasts and Cyanobacteria. Front Plant Sci 9:206. https://doi.org/10.3389/fpls.2018.00206
Kongjaimun A, Kaga A, Tomooka N, Somta P, Shimizu T, Shu Y, Isemura T, Vaughan DA, Srinives P (2012) An SSR-based linkage map of yardlong bean (*Vigna unguiculata* (L.) Walp. subsp. *unguiculata* Sesquipedalis Group) and QTL analysis of pod length. Genome 55:81–92
Konieczny A, Ausubel FM (1993) A procedure for mapping Arabidopsis mutations using co-dominant ecotype-specific PCR-based markers. Plant J. 4(2):403–410
Kosambi DD (1944) The estimation of map distance from recombination values. Ann Eugen 12:172–175
Laksana C, Chanprame S (2015) A simple and rapid method for RNA extraction from young and mature leaves of oil palm (*Elaeis guineensis* Jacq.). J ISSAAS 21:96–106
Legendre L, Rueter S, Heinstein PF, Low PS (1993) Characterization of the oligogalacturonide-induced oxidative burst in cultured soybean (*Glycine max*) cells. Plant Physiol 102:233–240
Lemarie A, Huc L, Pazarentzos E, Mahul-Mellier AL, Grimm S (2011) Specific disintegration of complex II succinate: ubiquinone oxidoreductase links pH changes to oxidative stress for apoptosis induction. Cell Death Differ 18:338–349
Leslie ME, Rogers SW, Heese A (2016) Increased callose deposition in plants lacking DYNAMIN-RELATED PROTEIN 2B is dependent upon POWDERY MILDEW RESISTANT 4. Plant Signal Behav 11(11):e1244594. https://doi.org/10.1080/15592324.2016.1244594
Li H, Ye G, Wang J (2007) A modified algorithm for the improvement of composite interval mapping. Genetics 175:361–374
Li Z, Ding B, Zhou X, Wang GL (2017) The rice dynamin-related protein OsDRP1E negatively regulates programmed cell death by controlling the release of cytochrome c from mitochondria. PLoS Pathog 13(1):e1006157. https://doi.org/10.1371/journal.ppat.1006157
Livak KJ, Schmittgen TD (2001) Analysis of relative gene expression data using real-time quantitative PCR and the $2_T^{-\Delta\Delta C}$ method. Methods 25:402–408. https://doi.org/10.1006/meth.2001.1262
Lodhi MA, Ye GN, Weeden NF, Reisch BI (1994) A simple and efficient method for DNA extraction from grapevine cultivars and *Vitis* species. Plant Mol Biol Rep 12:6–13
Lonardi S, Muñoz-Amatriaín M, Liang Q, Shu S, Wanamaker SI, Lo S et al (2019) The genome of cowpea (*Vigna unguiculata* [L.] Walp.). Plant J 98:767–782
Meng L, Li H, Zhang L, Wang J (2015) QTL IciMapping: integrated software for genetic linkage map construction and quantitative trait locus mapping in biparental populations. Crop J 3:269–283
Mhamdi A, Noctor G (2016) High CO_2 primes plant biotic stress defenses through redox-linked pathways. Plant Physiol 172:929–942
Muñoz-Amatriaín M, Mirebrahim H, Xu P, Wanamaker SI, Luo MC et al (2017) Genome resources for climate-resilient cowpea, an essential crop for food security. Plant J 89:1042–1054. https://doi.org/10.1111/tpj.13404
Murphy MP (2009) How mitochondria produce reactive oxygen species. Biochem J 417:1–13. https://doi.org/10.1042/BJ20081386
Neff MM, Neff JD, Chory J, Pepper AE (1998) dCAPS, a simple technique for the genetic analysis of single nucleotide polymorphisms: experimental applications in *Arabidopsis thaliana* genetics. Plant J 14:387–392
Neff MM, Turk E, Kalishman M (2002) Web-based primer design for single nucleotide polymorphism analysis. Trends Genet 18:613–615
Oblessuc PR, Matiolli CC, Chiorato AF, Camargo LEA, Benchimol-Reis LL, Melotto M (2015) Common bean reaction to angular leaf spot comprises transcriptional modulation of genes in the *ALS10.1* QTL. Front Plant Sci 6:152. https://doi.org/10.3389/fpls.2015.00152
Park SY, Choi J, Lim SE, Lee GW, Park J, Kim Y et al (2013) Global expression profiling of transcription factor genes provides new insights into pathogenicity and stress responses in the rice blast fungus. PLoS Pathog 9(6):e1003350. https://doi.org/10.1371/journal.ppat.1003350
Peng J, Ronin Y, Fahima T, Röder MS, Li Y, Nevo E, Korol A (2003) Domestication quantitative trait loci in *Triticum dicoccoides*, the progenitor of wheat. Proc Natl Acad Sci USA 100:2489–2494
Schertl P, Braun HP (2014) Respiratory electron transfer pathways in plant mitochondria. Front Plant Sci 5:163. https://doi.org/10.3389/fpls.2014.00163
Schneider RW, Williams RJ, Sinclair JB (1976) Cercospora leaf spot of cowpea: models for estimating yield loss. Phytopathology 66:384–388
Singh BB (2005) Cowpea [*Vigna unguiculata* (L.) Walp]. In: Singh RJ, Jauhar PP (eds) Genetic resources, chromosome engineering and crop improvement, vol 1. CRC Press, Boca Raton, pp 117–162
Singh R, Dangol S, Chen Y, Choi J, Cho YS, Lee JE, Choi MO, Jwa NS (2018) *Magnaporthe oryzae* effector AVR-Pii helps to establish compatibility by inhibition of the rice NADP-malic enzyme resulting in disruption of oxidative burst and host innate immunity. Mol Cells 39:426–438
Smith JM, Leslie ME, Robinson SJ, Korasick DA, Zhang T, Backues SK, Cornish PV, Koo AJ, Bednarek SY, Heese A (2014) Loss

of *Arabidopsis thaliana* dynamin-related protein 2b reveals separation of innate immune signaling pathways. PLoS Pathog 10(12):e1004578. https://doi.org/10.1371/journal.ppat.1004578

Tang D, Ade J, Frye CA, Innes RW (2006) A mutation in the GTP hydrolysis site of Arabidopsis dynamin-related protein 1E confers enhanced cell death in response to powdery mildew infection. Plant J 47:75–84. https://doi.org/10.1111/j.1365-313X.2006.02769.x

Temnykh S, DeClerck G, Lukashova A, Lipovinch L, Cartinhour S, McCouch S (2001) Xomputational and experimental analysis of microsatellites in rice (*Oryza sativa* L.): Frequency, length variation, transposon association and genetic marker potential. Genome Res 11:1441–1452

Tenhaken R, Levine A, Brisson LF, Dixon RA, Lamb C (1995) Function of the oxidative burst in hypersensitive disease resistance. Proc Natl Acad Sci USA 92(10):4158–4163

Torres MA (2010) ROS in biotic interactions. Physiol Plant 138:414–429. https://doi.org/10.1111/j.1399-3054.2009.01326.x

Untergasser A, Cutcutache I, Koressaae T, Ye J, Faircloth BC, Remm M, Rozen SG (2012) Primer3-new capabilities and interfaces. Nucl Acids Res 40:e115. https://doi.org/10.1093/nar/gks596

Van Os H, Stam P, Visser RG, Van Eck HJ (2005) RECORD: a novel method for ordering loci on a genetic linkage map. Theor Appl Genet 112:30–40

Voll LM, Zell MB, Engelsdorf T, Saur A, Wheeler MG, Drincovich MF, Weber AP, Maurino VG (2012) Loss of cytosolic NADP-malic enzyme 2 in *Arabidopsis thaliana* is associated with enhanced susceptibility to *Colletotrichum higginsianum*. New Phytol 195:189–202. https://doi.org/10.1111/j.1469-8137.2012.04129.x

Winning BM, Bourguignon J, Leaver CJ (1994) Plant mitochondrial NAD^+-dependent malic enzyme. cDNA cloning, deduced primary structure of the 59- and 62-kDa subunits, import, gene complexity and expression analysis. J Biol Chem 269:4780–4786

Wu G, Cui X, Chen H, Renaud JB, Yu K, Chen X, Wang A (2018) Dynamin-like proteins of endocytosis in plants are coopted by potyviruses to enhance virus infection. J Virol. https://doi.org/10.1128/JVI.01320-1

Zhou H, Liu S, Yang C (2012) Over-expression of a NAD-malic enzyme gene from rice in *Arabidopsis thaliana* confers tolerances to several abiotic stresses. Adv Mater Res 393–395:863–866. https://doi.org/10.4028/www.scientific.net/AMR.393-395.863